meats marketed in North-East India. *Proc. Natl. Acad. Sci., India, Sect. B*, 2013, **84**(2), 337–342.
27. Kumar, R., Nongkhlaw, M., Acharya, C. and Joshi, S. R., Growth media composition and heavy metal tolerance behaviour of bacteria characterized from the sub-surface soil of uranium rich ore bearing site of Domiasiat in Meghalaya. *Indian J. Biotechnol.*, 2013, **12**, 115–119.
28. Bhattacharjee, K. and Joshi, S. R., Phylogenetic rearrangement of *Streptomyces* spp. on the basis of internal transcribed spacer (ITS) region using molecular morphometrics approach. *Indian J. Biotechnol.*, 2013, **12**, 67–79.
29. Kumar, R., Nongkhlaw, M., Acharya, C. and Joshi, S. R., Bacterial community structure from the perspective of the uranium ore deposits of Domiasiat in India. *Proc. Natl. Acad. Sci., India, Sect. B*, 2013, **83**(4), 485–497.
30. Devi, L. S., Bareh, D. A. and Joshi, S. R., Studies on biosynthesis of antimicrobial silver nanoparticles using endophytic fungi isolated from the ethno-medicinal plant *Gloriosa superba* L. *Proc. Natl. Acad. Sci., India, Sect. B*, 2013; DOI:10.1007/s40011-013-0185-7.
31. Bhattacharjee, K., Banerjee, S., Bawitlung, L., Krishnappa, D. and Joshi, S. R., A study on parameter optimization for degradation of endosulfan by bacterial consortia isolated from contaminated soil. *Proc. Natl. Acad. Sci., India, Sect. B*, 2013; DOI: 10.1007/s40011-013-0223-5.
32. Khaund, P. and Joshi, S. R., Wild edible macrofungal species consumed by the Khasi tribe of Meghalaya, India. *Indian J. Nat. Prod. Resour.*, 2013, **4(2)**, 179–204.
33. Fenella, M. W. N. and Joshi, S. R., Micrographical assessment of antifungal effect of endophytic bacteria. *Proc. Natl. Acad. Sci., India, Sect. B*, 2014; DOI:10.1007/s40011-014-0321-z.
34. Fenella, M. W. N. and Joshi, S. R., Distribution pattern analysis of epiphytic bacteria on ethnomedicinal plant surfaces: a micrographical and molecular approach. *J. Microsc. Ultrastruct.*, 2014; DOI:10.1016/j.jmau.2014.02.003.
35. Bhattacharjee, K. and Joshi, S. R., NEMiD: A web-based curated microbial diversity database with geo-based plotting. *PLoS ONE*, **9**(4), e94088.

Received 27 May 2014; revised accepted 18 January 2015

The May 21st, 2014 Bay of Bengal earthquake: implications for intraplate stress regime

A. K. Rai[1,*], S. Tripathy[1] and S. C. Sahu[2]
[1]School of Earth, Ocean and Climate Sciences,
Indian Institute of Technology Bhubaneswar,
Bhubaneswar 751 007, India
[2]India Meteorological Department, Bhubaneswar 751 020, India

The northeastern part of the Indian Ocean, i.e. the Bay of Bengal (BoB) is located near some of the most complicated tectonic zones on the Earth. An earthquake of magnitude ~6.0 occurred on 21 May 2014 near the coast of Odisha. Occasional moderate to large earthquakes in BoB highlight the need to study precise hypocentre locations, and focal mechanisms to understand the cause of intraplate seismicity in BoB. It is also important for seismic hazard and tsunami risk evaluation along the eastern coast of India. We present an analysis of the digital data of this earthquake recorded by regional and global networks of seismic stations. Our analysis of travel-times of *P*- and *S*-waves indicates that the epicentre of the earthquake is located between the Eighty Five East and Ninety East ridges. The focus of this earthquake was at a depth of ~61 km, well below the lower boundary of the oceanic crust. The focal mechanism determined by modelling long period *P*- and *SH*-waveforms suggest an strike–slip motion along a NW–SE or NEE–SWW-directed fault or fracture. We interpret that the upper part of the BoB lithosphere is abnormally strong and brittle.

Keywords: Earthquake location, focal mechanism, intraplate seismicity, tectonic zones.

THE Indian Ocean is one of the most seismically active oceanic regions where intraplate seismicity is observed frequently[1] (Figure 1). The northeastern part of Indian

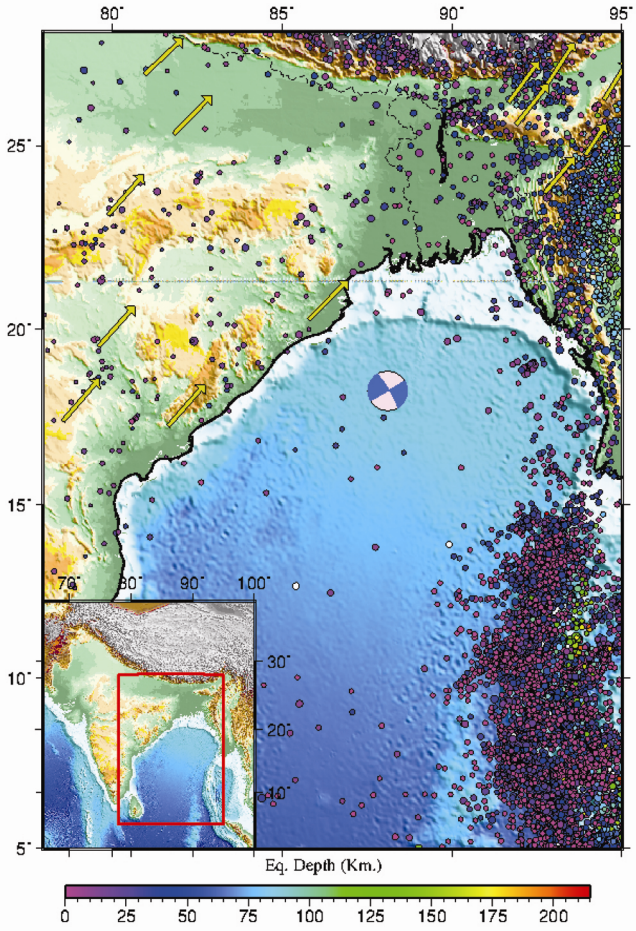

Figure 1. The location map and regional seismicity of the Bay of Bengal. The coloured circles represent earthquakes, where colour and size of a circles correspond to the depth, and magnitude of the earthquakes. Location of the 21 May 2014 earthquake is shown by beachball. Arrows show GPS velocity vectors[33].

*For correspondence. (e-mail: akrai@iitbbs.ac.in)

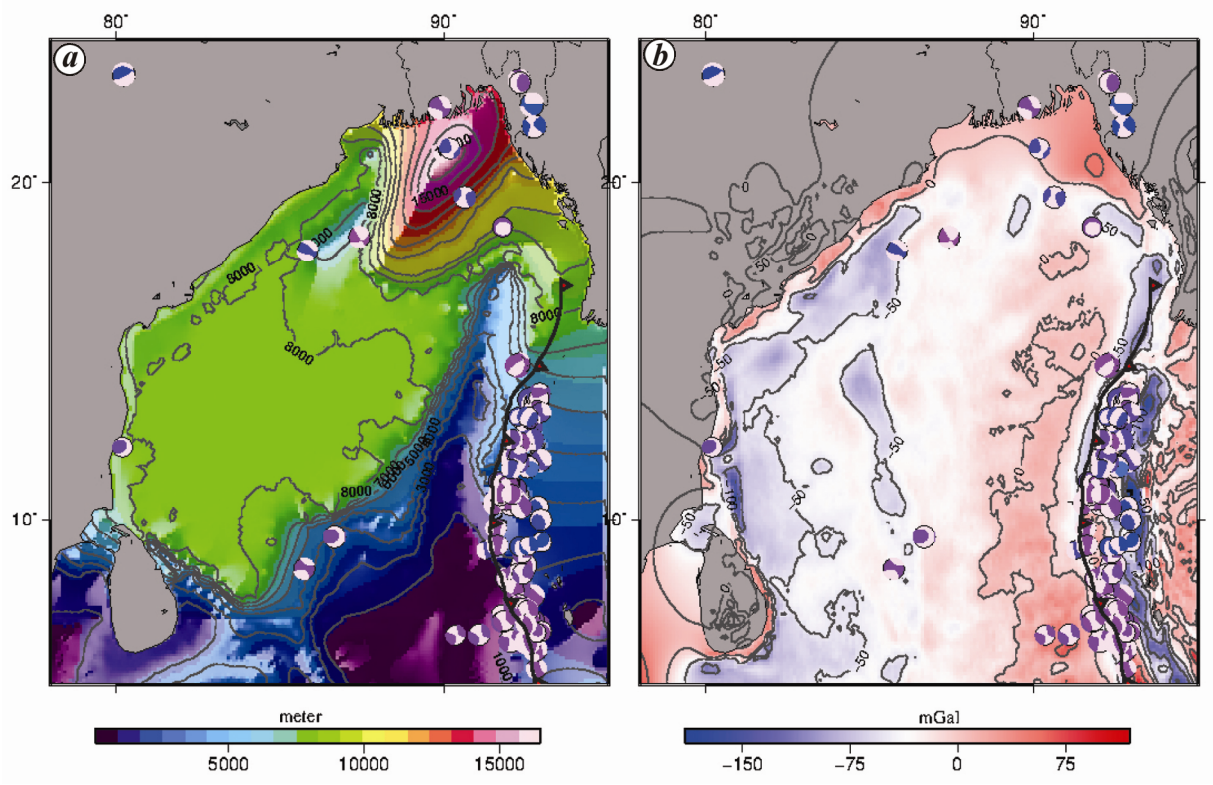

Figure 2. (***a***) The thickness of sediments[2] and (***b***) free-air gravity anomaly[34] maps of the Bay of Bengal.

Ocean, i.e. the Bay of Bengal (BoB) is unique among the world's oceanic basins, having ~8–16 km thick young sedimentary deposits[2] derived from rapid erosion of the Himalayan mountains by large rivers such as the Ganga and Brahmaputra[3,4]. The sedimentary thickness increases up to 16 km near the delta of the two rivers (Figure 2 *a*). Furthermore, BoB is located near the junction of some of the most complex tectonic features on the earth[4–6]. It is surrounded by the Shillong Plateau in the north, the Indo-Burmese arc in the NE, the Andaman–Sumatra subduction zone in the SE[7–11] and the Eastern Ghats Mobile Belt (EGMB) in the west[11–13]. Besides these, the seafloor of BoB is traversed by numerous faults, fracture zones and ridges of volcanic origin predominantly aligned in the NS and NNE–SSW directions[14].

The lithosphere of the BoB evolved during the early Cretaceous break-up of eastern Gondwanaland and experienced three major phases of seafloor spreading. Most of the BoB crust was formed during long normal magnetic polarity period[6,14,15]. The major morphological features such as the Eighty Five East, and Ninety East ridge (NER) bathymetric high are visibly traceable up to 10°N latitude, but disappear beneath the thick sediments at northern latitudes. However, traces of these ridges are clearly evident on the gravity anomaly map up to 20°N latitudes (Figure 2 *b*). Efforts are continuously being made by various national and international research groups to determine the high-resolution crustal structure of BoB[4,6,16]. On the basis of earthquake data, Brune and Priestley[16], and Brune and Singh[17] estimated a continent-like thick crust in BoB, whereas recent analysis of gravity data predicted relatively thin crust for few regions[15]. Detailed knowledge of the deep seismic structure of BoB by active seismic methods is primarily hindered by thick sedimentary cover.

Historically only few large earthquakes have been noted in various parts of BoB[1,8,18]. The cause of intraplate seismicity in BoB is poorly understood, primarily because of sparse distribution of regional earthquake recording stations, and unknown crustal structure. Most parts of the two volcanic ridges are considered aseismic; however, focal mechanism of few earthquakes near NER shows a NE–SW compression, where a combination of thrust and strike–slip motion occurs[8,19,20]. GPS observations indicate differential motion between various tectonic boundaries in NE India[21]. Part of this differential motion is likely to be accommodated at fractures zones in BoB.

To better understand tectonics and the prime cause of earthquakes in a region, it is important to locate them with high accuracy, besides correctly modelling focal mechanisms. The precision of hypocentre determination depends on good azimuthal and epicentral distribution of seismological stations around the source region, and accurate velocity model. Accurate estimates of source parameters are also important for understanding seismic

and tsunami hazard risks, and assessment of peak ground motion which critically depends on the depth of the earthquakes. Furthermore, in the absence of any other indicator of stress, the earthquake focal mechanisms provide an indirect estimate of state of stress in the lithosphere. Earthquake bulletins that are routinely published by the International Seismic Center (ISC), the National Earthquake Information Center (NEIC), and the United States Geological Survey (USGS) are mostly determined by automatic processing of a large set of data, and occasionally verified manually. However, automatic estimates of source parameters may be affected by inherent trade-off between origin time and focal depth, and may have significant errors in hypocentre parameters.

The recent earthquake of magnitude ~6.0 that occurred on 21 May 2014 in BoB was recorded by the Global Digital Seismograph Network (GDSN; Figure 3). This provides an opportunity to determine the hypocentre and source parameters of this moderate to large magnitude earthquake, and understand the cause of intraplate seismicity in BoB. We present analysis of seismograms recorded by a network of international broadband seismometers distributed at local, regional and teleseismic distances, and determine the hypocentre parameters and fault plane solution.

The 21 May 2014 earthquake was large enough ($M \sim 6.0$) to be recorded by the seismological observatories located around the source region. The digital waveform data were obtained from the Data Management Center (DMC) of Incorporated Research Institutions for Seismology (IRIS), and International Federation of Digital Seismograph Network (FDSN; Figure 3). Besides we also used data from the nearest stations of India Meteorological Department (IMD) located ~300 km from the epicentre of the earthquake (Figure 4). The data were converted to standard seismological processing formats[22,23]. The data analysis technique is described in detail below.

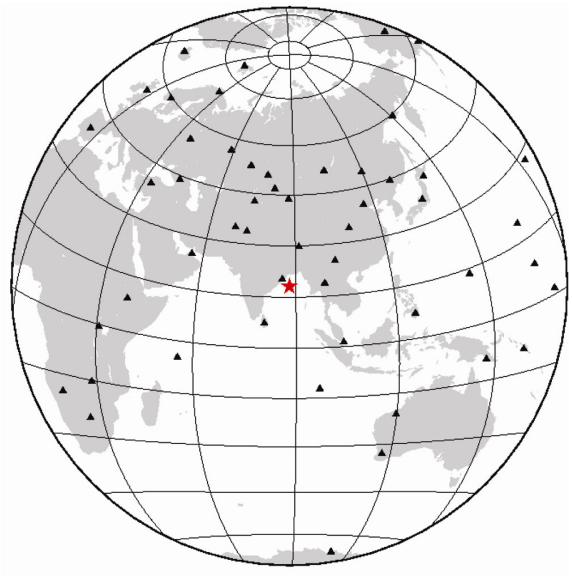

Figure 3. Locations of the seismic stations whose data were used. The epicentre of the 21 May 2014 earthquake is shown by a red star.

We use the preliminary hypocentre locations reported by various reporting agencies (Table 1) to identify the seismic phases on the data. Travel-times of *P*- and *S*-phases were manually picked on vertical and horizontal components of the seismograms. The uncertainties of the travel-time picks are of the order of sampling interval (0.02 sec) of the data. The hypocentre determination of earthquake requires an accurate prediction of travel-times through the model. Therefore, a realistic velocity model is needed for the source region. Crustal-scale high-resolution seismic velocity models for BoB are unavailable in the public domain. Therefore, in this study we use the velocity model (Figure 5) that is extracted from a recent global compilation of lithospheric structure (LITHO-1.0) of the earth[24]. The velocity model was slightly modified for variations in the thickness of sediments in the source region. A recent compilation of global sediment thickness dataset was used for this purpose[2]. The *P*- and *S*-wave travel-time data (Figure 6 *a* and *b*) were transformed into appropriate format required to determine the hypocentre parameters[25,26]. The travel-times of seismic waves to any point in the model can be easily calculated. The misfit between the observed and computed travel-times can be minimized over a grid-search to find the best possible values of hypocentre parameters in space (minimum misfit solution). For example, by minimizing the least squared misfit for n observations given by $r_i = (t_i^{\text{obs}} - t_0) - t_i^{\text{cal}}$, it is possible to estimate best value of t_0 in an average sense for several observations. The least square approach is a commonly used method where we minimize the sum of the squared residuals e for n observations, where $e = \sum_{i=1}^{n} (ri)^2$.

Then, the root mean squared (RMS) residual[22] can be written as $\sqrt{(e/n)}$. A similar approach provides an estimate of latitude, longitude and depth of the earthquake for the minimum value of e. The travel-time picks of *P*- and *S*-phases were categorized into best, good and poor quality. Full weights were assigned to best available data, whereas good and poor quality data were assigned a weight of 0.7 and 0.3 respectively, while determining locations. Travel-time data were randomly selected from the database, and hypocentre parameters were determined for several sets. This bootstrap methodology provides a better estimate of uncertainty in parameters and their dependence on data quality. The grid-search estimates for latitude and longitude of the earthquake (Figure 6 *c*) indicate that the solutions are robust within the error bounds, whereas a search for depth of the earthquake indicates a minimum misfit solution of ~61 km (Figure 6 *d*). The depth was further constrained by comparing travel-times of depth-reflected phases[27] such as *pP*.

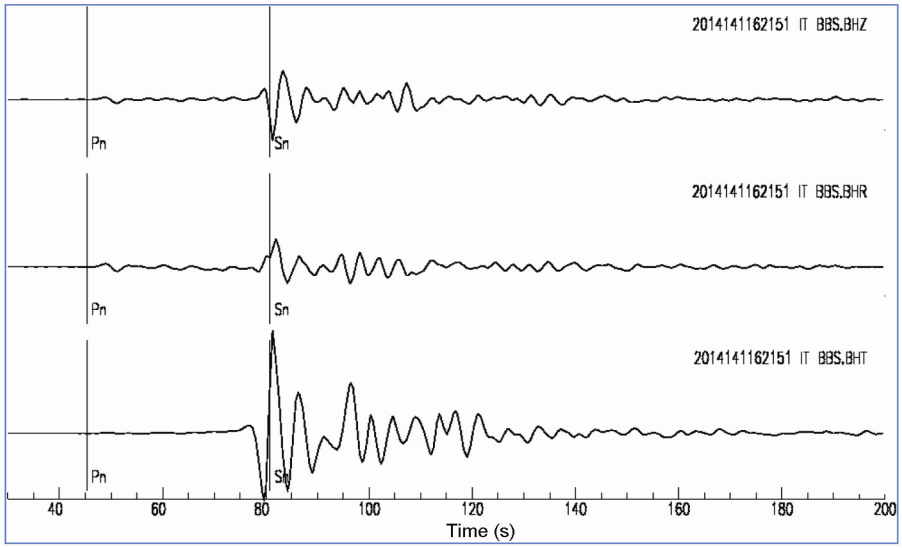

Figure 4. Vertical, radial and transverse component seismograms recorded at the nearest (~300 km) station, Bhubaneswar.

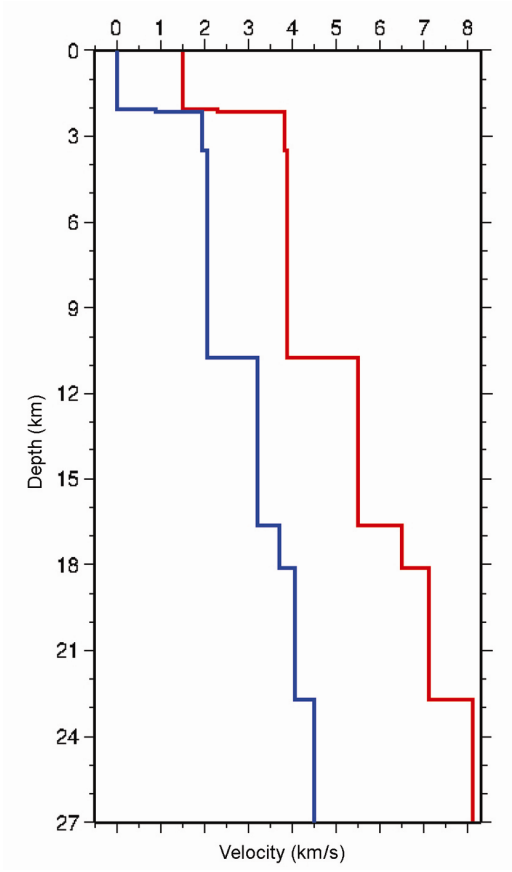

Figure 5. Source side velocity model (modified from Pasyanos *et al.*[24]) used for locating and computing focal mechanism of the 21 May 2014 Bay of Bengal earthquake.

To determine the fault plane solution (strike, dip and rake) and relative amplitude of the triangular source time function, we used long-period teleseismic body-waveform modelling technique[28,29]. The digital waveform data of *P*-phases from stations located at a distance range 30°–90°, and *SH*-waveform from stations located at an epicentral distance of 30°–70° were used for modelling. The method assumes that the earthquake source can be approximated as a point source (the centroid) in space. The time history of the displacement on the fault is represented by a source-time function made up of a series of overlapping isosceles triangles whose number and duration can be determined by waveform fits. The teleseismic data were obtained from GDSN. The instrument response was deconvolved from the seismograms and converted to WWLLN form.

An attenuation correction was employed using Futterman's operator[30] with $t^* = 1$s for *P*- and $t^* = 4$s for *SH*-waves. Before inversion, records were bandpass-filtered with corner frequencies at 0.01 and 0.12 Hz to remove the high-frequency components and were integrated to displacement. To compute synthetic seismograms we used a two-layer model with a half-space with velocities 6.5 and 3.7 km/s for *P*- and *S*-waves respectively, and density of 2.8 gm/cc, under lying a water layer depth of 2.07 km. This model is adequate to explain the low frequency content of the teleseismic waveforms at distances between 30° and 90° due to the simplicity of the earth layer structure at the same distance range.

The inversion slowly adjusts the relative amplitude of the source-time function elements, centroid depth, seismic moment and source orientation (strike, dip and rake) by minimizing the misfit between observed and synthetic seismograms. We prefer the visually optimum solution as minimum misfit solution. The optimum focal mechanism derived from waveform fit is based on ~30 *P*- and *SH*-waveforms with good azimuthal and epicentral distribution around the source. The covariance matrix associated

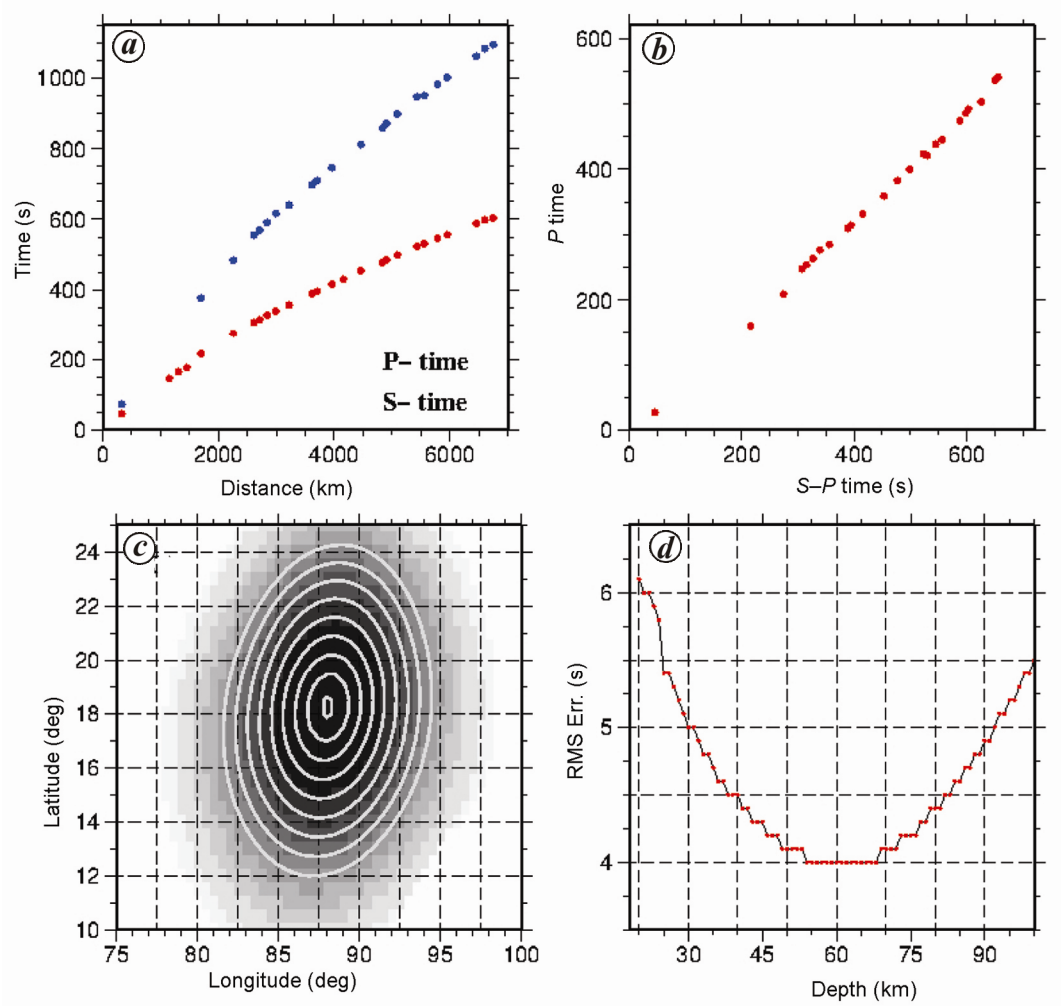

Figure 6. Travel-time data and earthquake location. ***a***, *P*- and *S*-wave travel-time data; ***b***, Plot of *P*- versus *S*–*P* travel-times; ***c***, Contour map of minimum misfit latitude–longitude of earthquake; ***d***, Minimum misfit depth of earthquake.

Table 1. Source parameter reported by various agencies

Agency	Origin time (GMT)	*M*	Latitude (°N)	Longitude (°E)	Depth (km)	Strike	Dip	Rake
IMD	21 May 2014. 16:21:50.0	6.0	18.3	87.90	10	–	–	–
INCOIS	21 May 2014, 16:21:51.0	5.8	18.24	87.95	5	–	–	–
USGS	21 May 2014, 16:21:54.0	5.9 (*Mw*)	18.20	88.02	44.3	–	–	–
GCMT	21 May 2014, 16.21.57.8	6.1 (*Mw*)	18.08	88.07	59.7	323/53	83/88	178/7
Geoscope	21 May 2014, 16:21:54.0	6.09 (*Mw*)	18.254	88.08	48	321/231	82/90	–180/–8
This study	21 May 2014, 16:21:55.4	5.7 (*Mb*) ± 3	18.26 ± 0.5	88.10 ± 0.5	61 ± 6	69 ± 5	83 ± 5	7 ± 5

with the minimum misfit solution often underestimates the true uncertainties associated with the source parameters. In order to determine realistic uncertainties, we fixed some of the source parameter values close to, but slightly different from those of the minimum misfit values and allowed other parameters to change in the inversion. The visual examination of the fits of the observed and synthetic seismograms is an important criterion for an optimal solution. The minimum misfit model that was obtained by inversion of teleseismic long-period waveform data suggests that the earthquake took place due to strike–slip motion along either a NW–SE or a NEE–SWW directed fault. The detailed modelling results are shown in Figure 7.

The seismicity of BoB is still not well understood, primarily due to lack of adequate instrumentation at local and regional scales. A moderate to large earthquake of magnitude $M \sim 6.0$ that occurred in BoB on 21 May 2014 was felt across Odisha, and was well recorded by the global network of seismological stations. We used the

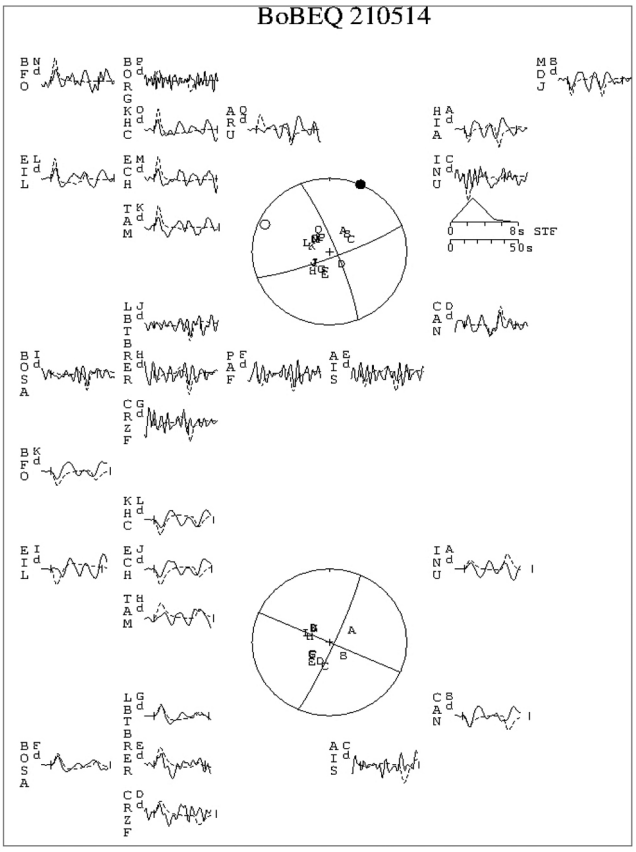

Figure 7. *P*- and *SH*-waveform modelling of the 21 May 2014 Bay of Bengal earthquake. Minimum misfit solution is shown (strike–69, dip–83, rake–7, depth–61 km). Individual waveforms are shown at their approximate azimuths around the focal sphere appropriate to their phase (*P* – at the top, *SH* – at the bottom showing lower hemispherical projections), designated by station abbreviation. The observed and synthetic data are shown by solid and dashed lines. The employed source time function (STF), and the waveform timescale are depicted at the centre of the figure. On the focal sphere solid dot denotes *P*-axis and open circle denotes *T*-axis.

digital waveform data recorded by the GDSN network located at local and regional distances and relocated the hypocentre of the earthquake, and determined the fault-plane solution by modelling the teleseismic long-period *P*- and *SH*-waveforms. Our analysis indicates that the earthquake occurred at a depth of ~61 km, well below the suggested lower boundary of the crust, i.e. Moho. Furthermore, the waveform inversion indicates that the earthquake could have occurred along a NW–SE or NEE–SWW-oriented fault in a near strike–slip motion. Recent studies suggest that the observed seismicity in the recent past in the high-grade EGMB may be due to reactivation of ancient faults[31]. There is good possibility that these ancient faults may be extending towards BoB and are experiencing stress build-up due to intraplate differential motion as indicated by GPS studies. We propose that moderate to large intraplate earthquakes in BoB with a strike–slip motion may be an indication of rejuvenated neo-tectonic activity due to differential motion at the eastern and northeastern boundary of the Indian plate that is being accommodated along palaeo-faults and fractures in BoB related to India–Antarctica–Australia separation. We interpret the deep intraplate seismicity of BoB due to abnormal mechanical strength of the upper part of the lithosphere. On the basis of gravity analysis, modelling sediment deposition and effective elastic thickness of the lithosphere, RadhaKrishna *et al.*[15] suggested that BoB lithosphere could have gained strength during sedimentation. The brittle strength of the upper lithosphere may also increase significantly due to percolation of sea water to greater depths through numerous faults and fractures that traverse the bathymetry of the northern Indian Ocean.

1. Andrade, V. and Rajendran, K., The April 2012 Indian Ocean earthquakes: seismotectonic context and implications for their mechanisms. *Tectonophysics*, 2014, **617**, 126–139.
2. Whittaker, J. M., Goncharov, A., Williams, S. E., Muller, R. and Leotchenkov, G., Global sediment thickness dataset updated for the Australian–Antarctic Southern Ocean. *Geochem. Geophys. Geosyst.*, 2013, **14**, 3297–3305.
3. Curray, J., Emmel, F., Moore, D. and Raitt, R., Structure, tectonics, and geological history of the northeastern Indian ocean. In *The Ocean Basins and Margins* (eds Nairn, A. E. M. and Stehli, F. G.), 1982, vol. 6, pp. 399–450.
4. Rao, D. G., Krishna, K. and Sar, D., Crustal evolution and sedimentation history of the Bay of Bengal since the Cretaceous. *J. Geophys. Res.*, 1997, **102**, 17747–17768.
5. Rao, T. and Rao, B., Some structural features of the Bay of Bengal. *Tectonophysics*, 1986, **124**, 141–153.
6. Krishna, K., Michael, L., Bhattacharyya, R. and Majumdar, T., Geoid and gravity anomaly data of conjugate regions of Bay of Bengal and Enderby Basin: new constraints on breakup and early spreading history between India and Antarctica. *J. Geophys. Res.*, 2009, **114**, doi:10.1029/2008JB005808.
7. Angelier, J. and Baruah, S., Seismotectonics in Northeast India: a stress analysis of focal mechanism solutions of earthquakes and its kinematic implications. *Geophys. J. Int.*, 2009, **178**, 303–326.
8. Levchenko, O. V., Tectonic aspects of intraplate seismicity in the northeastern Indian Ocean. *Tectonophysics*, 1989, **170**, 125–139.
9. Wang, Y. *et al.*, Active tectonics and earthquake potential of the Maynmar region. *J. Geophys. Res.*, 2014, **119**; doi: 10.1002/2013JB10762.
10. Curray, J. R., Tectonics and history of the Andaman Sea region. *J. Atmos. Sci.*, 2005, **25**, 187–232.
11. Kundu, B. and Gahalaut, V. K., Tectonic geodesy revealing geodynamic complexity of the Indo-Burmese arc region, North East India. *Curr. Sci.*, 2013, **104**, 920–933.
12. Bhattacharya, S., Eastern Ghats granulite terrain of India: an overview. *J. South Asian Earth Sci.*, 1996, **14**, 165–174.
13. Chetty, T. R. K., Structural architecture of the northern composite terrane, the Eastern Ghats Mobile Belt, India: implications for Gondwana tectonics. *Gondwana Res.*, 2010, **15**, 565–582.
14. Das Gupta, A. B. and Mukherjee, B., *Geology of NW Bengal Basin*, Geological Society of India, 2006, pp. 57–143.
15. RadhaKrishna, M., Subrahmanyam, C. and Damodharan, T., Thin oceanic crust below Bay of Bengal inferred from 3-D gravity interpretation. *Tectonophysics*, 2010, **493**, 93–105.
16. Brune, J. and Priestley, K., Anomalous crustal structure beneath the Bay of Bengal and passive oceanic sedimentary basins. *Proc. Indian Acad. Sci.* (*Earth Planet. Sci.*), 1989, **98**, 25–30.

17. Brune, J. and Singh, D., Continent-like crustal thickness beneath the Bay of Bengal sediments. *Bull. Seismol. Soc. Am.*, 1986, **76**, 191–203.
18. Wiens, D. A., Stein, S., Demets, C., Gordon, R. G. and Stein, C., Plate tectonic models for Indian Ocean intraplate deformation. *Tectonophysics*, 1996, **132**, 37–48.
19. Stein, S. and Okal, E. A., Seismicity and tectonic of the Ninetyeast Ridge area: Evidence for internal deformation of the Indian plate. *J. Geophys. Res.*, 1978, **83**, 2233–2245.
20. Subrahmanyam, C., Gireesh, R., Chand, S., Kamesh Raju, K. A. and Rao, D. G., Geophysical characteristics of the Ninetyeast Ridge – Andaman island arc/trench convergent zone. *Earth Planet. Sci. Lett.*, 2008, **266**, 29–45.
21. Socquet, A., Vigny, C., Chamot-Rooke, N., Simons, W., Rangin, C. and Ambrosius, B., India and Sunda plates motion and deformation along their boundary in Myanmar determined by GPS. *J. Geophys. Res.*, 2006, **111**, B05406; doi:10.1029/2005JB003877.
22. Havskov, J. and Ottemoller, L., Seis An earthquake analysis software. *Seismol. Res. Lett.*, 1999, **70**, 532–534.
23. Goldstein, P., Dodge, M. and Firpo, L. M., SAC availability for IRIS Community. *IRIS Newsl.*, 2005.
24. Pasyanos, M., Masters, T., Laske, G. and Ma, Z., LITHO1.0: an updated crust and lithospheric model of the Earth. *J. Geophys. Res.*, 2014; doi: 10.1002/2013JB010626.
25. Lienert, B. R. E. and Havskov, J., A computer program for locating earthquakes both locally and globally. *Seismol. Res. Lett.*, 1995, **66**, 26–36.
26. Lienert, B. R. E., Berg, E. and Frazer, L. N., Hypocenter: an earthquake location method using centered, scaled, and adaptively least squares. *Bull. Seismol. Soc. Am.*, 1986, **76**, 771–783.
27. Engdahl, E. R., Hilst, R. V. D. and Buland, R., Global teleseismic earthquake relocation with improved travel times and procedures for depth determination. *Bull. Seismol. Soc. Am.*, 1998, **88**, 722–743.
28. McCaffrey, R. and Abers, J., SYN3: a program for inversion of teleseismic body wave form on microcomputers, Technical Report AFGL-TR-0099, Air Force Geophysical Laboratory, Hanscomb Air Force Base, Massachusetts, 1998.
29. McCaffrey, R., Abers, G. and Zwick, P., Inversion of teleseismic body waves. International Association of Seismology and Physics of the Earth's Interior, 1991, **3**, 81–166.
30. Futterman, W., Dispersive body waves. *J. Geophys. Res.*, 1962, **67**, 5279–5291.
31. Gupta, S., Mohanty, W. K., Mandal, A. and Misra, S., Ancient terrane boundaries as probable seismic hazards: a case study from the northern boundary of the Eastern Ghats Belt India. *Geosci. Front.*, 2014, **5**, 17–24.
32. Wessel, P. and Smith, W. H. F., New, improved version of the generic mapping tools released. *EOS Trans. AGU*, 1998, **79**, 579.
33. Mahesh, *et al*., Rigid Indian plate constraints from GPS measurements. *Gondwana Res.*, 2012, **22**, 1068–1072.
34. Sandwell, D. T. and Smith, W. H. F., Global marine gravity from retracked geosat and ers-1 altimetry: ridge segmentation versus spreading rate. *J. Geophys. Res.*, 2009, **114**, B01411.

ACKNOWLEDGEMENTS. We thank Incorporated Research Institutions for Seismology (IRIS), Data Management Center (DMC), Washington for providing earthquake waveform data. Figures were prepared using Generic Mapping Tools[32].

Received 28 June 2014; revised accepted 4 March 2015

The admissible tsunamigenic source region of 24 September 2013 land-based earthquake – application of backward ray tracing technique

Ch. Patanjali Kumar*, B. Ajay Kumar, E. Uma Devi, R. S. Mahendra, M. V. Sunanda, M. Pradeep Kumar, J. Padmanabham, S. Dipankar and T. Srinivasa Kumar

Indian National Centre for Ocean Information Services (INCOIS), Hyderabad 500 090, India

A minor tsunami of about 50 cm was generated along the coast of Qurayat near Makran subduction zone in the Arabian Sea due to the 24 September 2013 Pakistan earthquake of magnitude 7.6 M_w(mB), although its source was ~200 km far inland of the Makran trench. The real-time sea-level observation network in the Arabian Sea recorded minor tsunami arrivals. In an attempt to explain the mechanism of this unusual tsunami, we use backward ray tracing technique to map the admissible region of tsunamigenic source. Basically, in this technique the ray equations are integrated starting from the specific locations of tsunami observations, in all possible directions. The known travel time of the initial waves to the respective tide gauges and tsunami buoys is used in this method. Backward wave front is constructed by joining all end-points of the rays from each of the locations. The region where the envelope of all backward wave fronts converges is considered as the source of the tsunami, which is ~470 km from the earthquake epicentre with the location at 24.8 N and 61.5 E. The admissible region identified is an undersea section between Chabahar and Gwadar, where a mud island had appeared subsequent to this earthquake. Convergence of the tsunami source zone and location of the mud island suggest that the sudden uplift must have caused the tsunami.

Keywords: Backward ray tracing, earthquake, tsunami, subduction zone.

ON 24 September 2013 at 11:29 UTC, an earthquake of magnitude 7.6 M_w(mB) occurred ~200 km away from the Makran coast of Pakistan. It was located ~280 km NW of Karachi, 26.99 N and 65.52 E (location obtained by ITEWS auto-location software) with a hypocentral depth of 10 km (Figure 1). This earthquake triggered a tsunami that was recorded by various sea-level tide gauges along the coastal regions of the Arabian Sea and tsunami buoys in the Arabian Sea. Based on the global experiences, it is known that tsunamis are usually generated by undersea shallow-focus earthquakes. Co-seismic or delayed tsunami generation due to submarine landslides or slumps is

*For correspondence. (e-mail: patanjali@incois.gov.in)